BOILING HEAT TRANSFER MECHANISMS IN EARTH AND LOW GRAVITY: BOUNDARY CONDITION AND HEATER ASPECT RATIO EFFECTS

Jungho Kim
University of Maryland
Dept. of Mechanical Engineering
College Park, MD 20742

Boiling is a complex phenomenon where hydrodynamics, heat transfer, mass transfer, and interfacial phenomena are tightly interwoven. An understanding of boiling and critical heat flux in microgravity environments is of importance to space based hardware and processes such as heat exchange, cryogenic fuel storage and transportation, electronic cooling, and material processing due to the large amounts of heat that can be removed with relatively little increase in temperature. Although research in this area has been performed in the past four decades, the mechanisms by which heat is removed from surfaces in microgravity are still unclear. Recently, time and space resolved heat transfer data were obtained in both earth and low gravity environments using an array of microheaters varying in size between 100 microns to 700 microns. These heaters were operated in both constant temperature as well as constant heat flux mode.

Heat transfer under nucleating bubbles in earth gravity were directly measured using a microheater array with 100 μm resolution operated in constant temperature mode with low and high subcooled bulk liquid along with images from below and from the side. The individual bubble departure diameter and energy transfer were larger with low subcooling but the departure frequency increased at high subcooling, resulting in higher overall heat transfer. The bubble growth for both subcoolings was primarily due to energy transfer from the superheated liquid layer–relatively little was due to wall heat transfer during the bubble growth process. Oscillating bubbles and sliding bubbles were also observed in highly subcooled boiling. Transient conduction and/or microconvection was the dominant heat transfer mechanism in the above cases. A transient conduction model was developed and compared with the experimental data with good agreement.

Data was also obtained with the heater array operated in a constant heat flux mode and measuring the temperature distribution across the array during boiling. The instantaneous heat transfer into the substrate was numerically determined and subtracted from the supplied heat to obtain the wall to liquid heat flux. This data was then correlated with high speed (>1000Hz) visual recordings of the bubble growth and departure from the heater surface acquired through the bottom of the heater. The data indicated that microlayer evaporation and contact line heat transfer were not major heat transfer mechanisms for bubble growth, similar to the conclusions for constant wall temperature. The dominant heat transfer mechanism appeared to be transient conduction into the liquid as the liquid rewetted the wall during the bubble departure process.

Pool boiling heat transfer measurements from heaters of varying aspect ratio were obtained in low-g (0.01 g ±0.025 g) and high-g (1.7 g ±0.5 g) using the KC-135 aircraft. The heater aspect

ratio was varied by selectively powering arrays of heaters (2x2, 2x4, 2x6, 2x8, and 2x10) in a 10x10 heater array containing individual heaters 700x700 μm^2 in size. The liquid was degassed to an air concentration below 3 ppm by repeatedly pulling a vacuum on the vapor/gas above the liquid before measurements were made. The heat fluxes were generally observed to decrease as the heater aspect ratio increased. As the wall superheat increased, Marangoni convection appeared to increase and cause the large bubbles that formed on the heater to shrink, allowing liquid to rewet the surface, increasing the heat transfer. Why Marangoni convection was observed in what is essentially a fully degassed fluid is unclear, but may be due to contaminants or isomers within the fluid.

Boiling Heat Transfer Mechanisms in Earth and Low Gravity: Boundary Condition and Heater Aspect Ratio Effects

Jungho Kim
Dept. of Mechanical Engineering
University of Maryland
College Park, MD 20742

Acknowledgements

- **Undergraduate and graduate students**

  Chris Henry
  Vamsee Yerramilli
  John Benton
  Fatih Demiray
  Nagaraja Yaddanapuddi

- **NASA Personnel**

  John McQuillen (Grant monitor)
  Jerry Meyers (Constant heat flux results)
  Sam Hussey (Constant heat flux results)
  Glenda Yee (Constant heat flux results)
  John Yaniec

Overview

- **Introduction**

- **Earth gravity boiling mechanisms**

    –Constant wall temperature
    –Constant wall heat flux

- **Low gravity boiling mechanisms**

    –Heater size effects
    –Heater aspect ratio effects
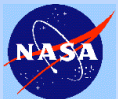
Introduction

Relevance to NASA's Mission
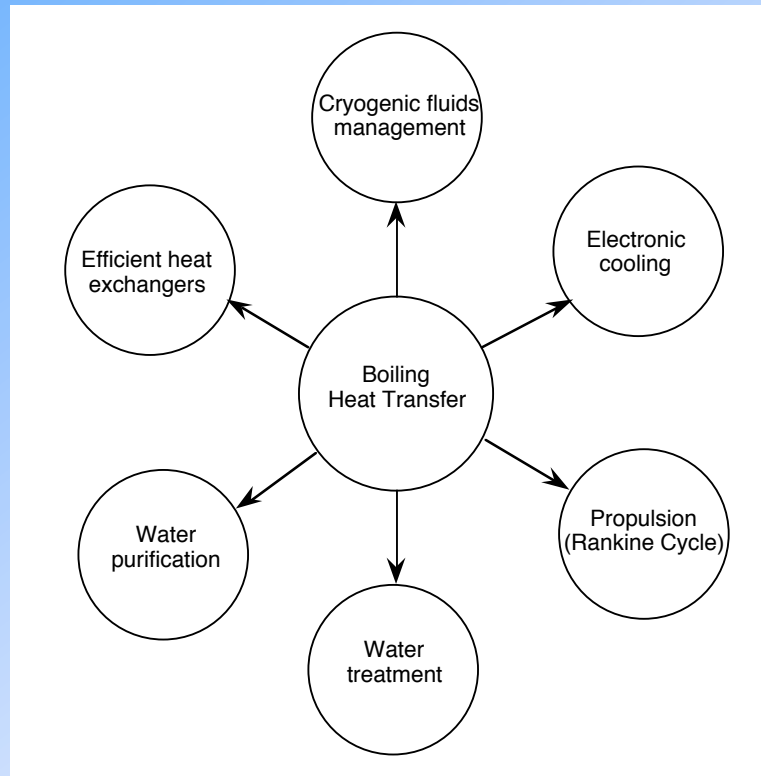
- **Provide fundamental understanding of gravity effects on boiling heat transfer mechanisms at various gravity levels so equipment and transfer processes can be designed efficiently.**

Model of Boiling: Mikic and Rosenhow (1969)

Growth of bubble
in superheated layer

D

2D

Bubble departure and
removalof superheated layer

Nucleation of new bubble
within superheated layer

Growth of new
superheated layer
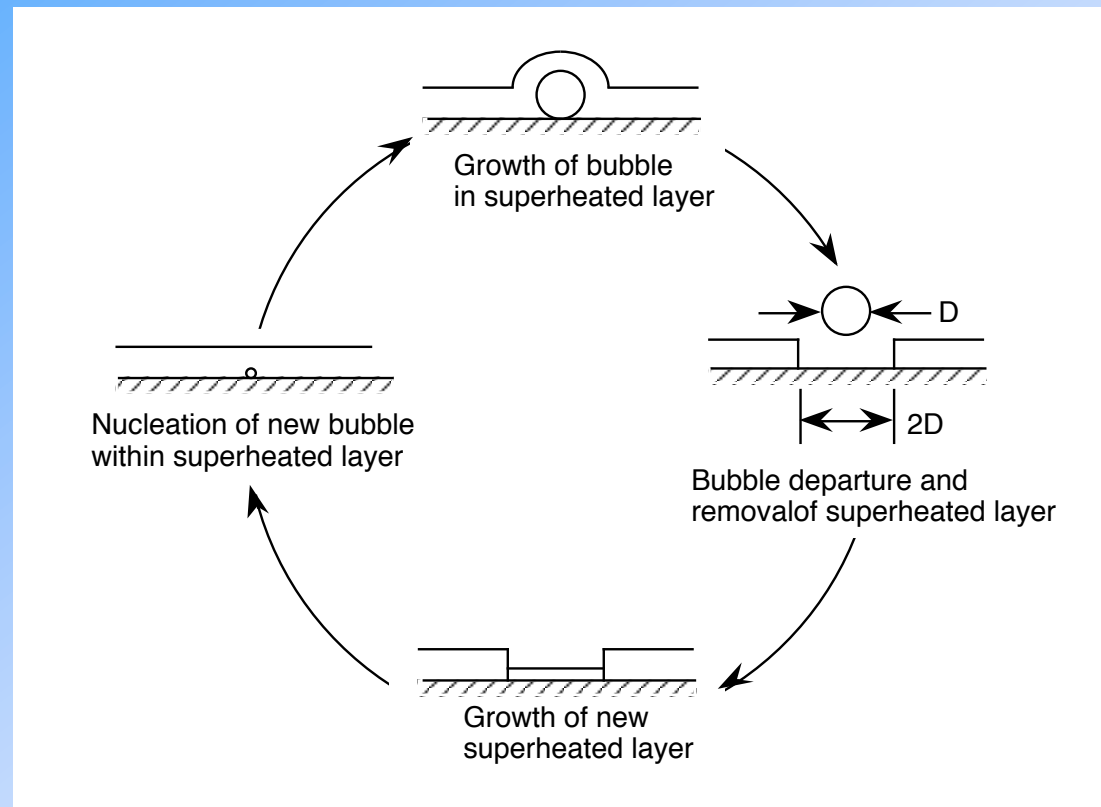
- **Heat transfer occurs primarily through conduction into liquid after bubble departs surface**

Model of Boiling: Microlayer Evaporation Model (Cooper and Lloyd–1969)

Liquid

Vapor

Wedge shaped "microlayer"
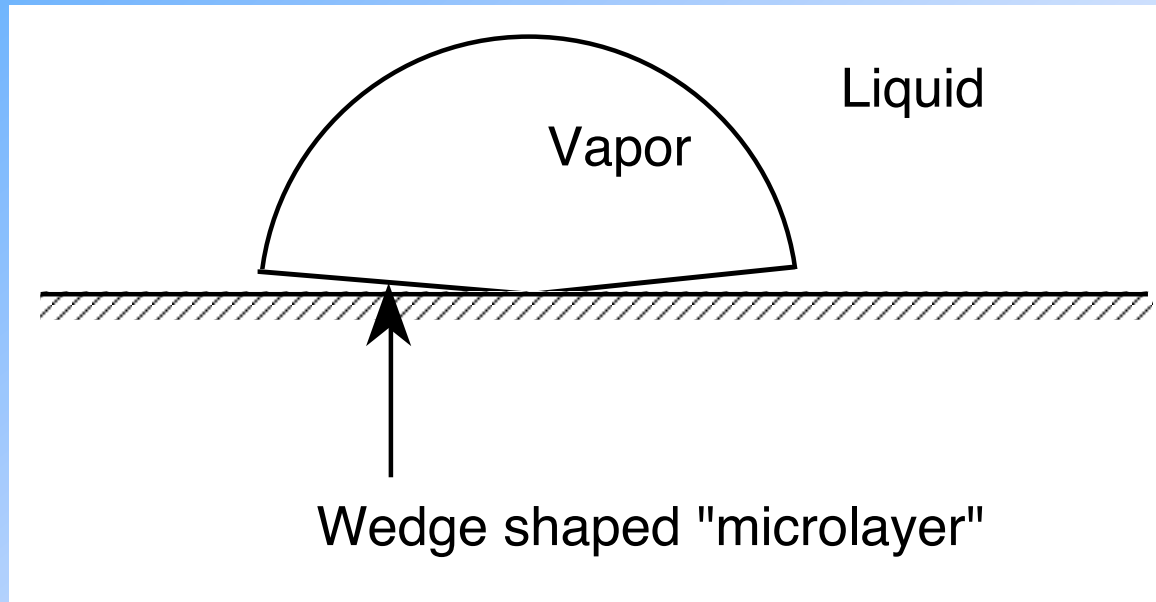
- **Heat transfer occurs primarily through evaporation of a thin film "microlayer" underneath bubble**

Model of Boiling: Contact Line Evaporation (Wayner, Stephan)
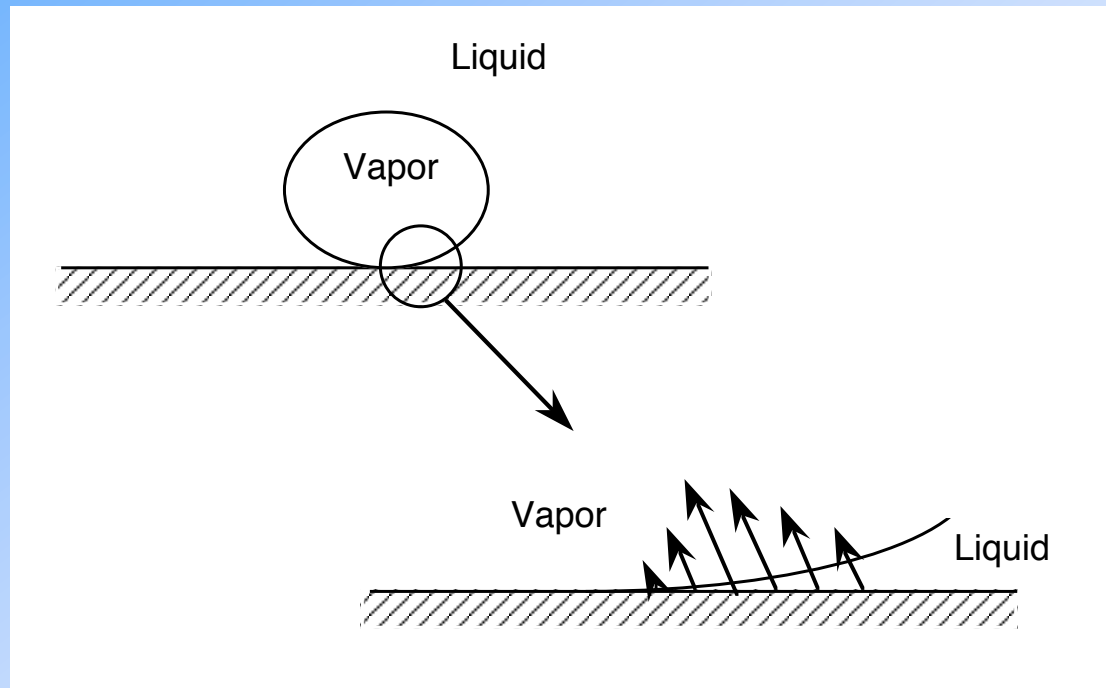
- **Heat transfer occurs primarily through conduction/evaporation of a thin meniscus at the three phase contact line**

Photograph of Heater Array
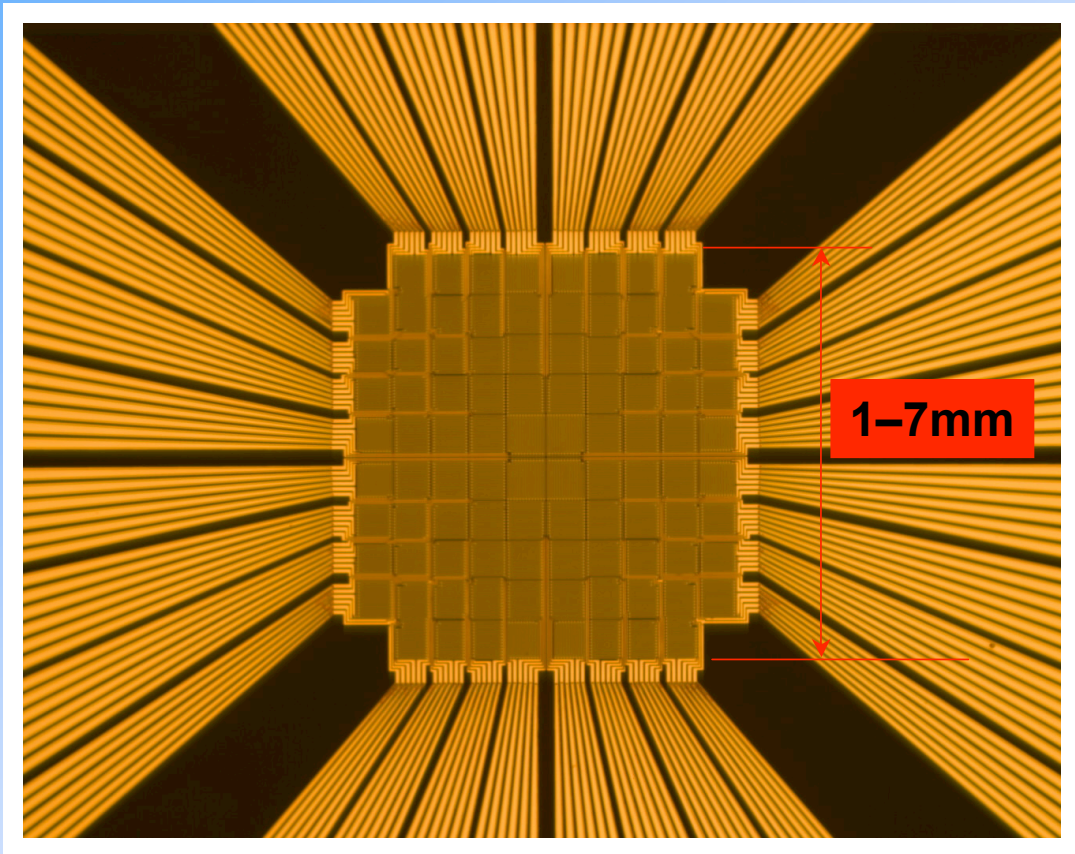
Feedback Control Circuit (Constant Temperature)
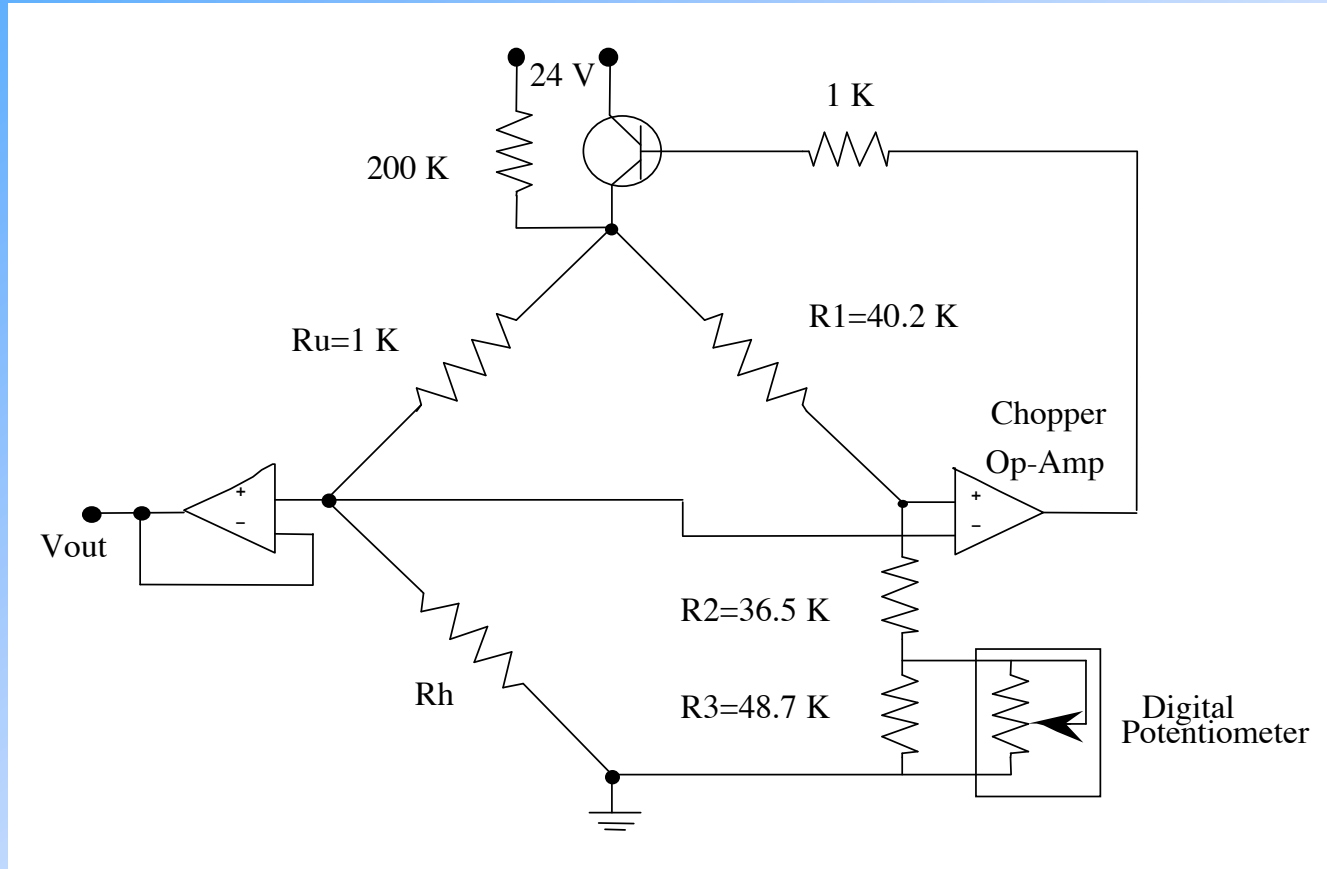
- **Feedback control circuit regulates heater temperature**
- **Frequency response up to 15 kHz.**

Schematic of Temperature Measuring Circuit (Constant Heat Flux)

V_{top}

R1   R2

V_{heater}

Amplifier → to multiplexer

Rh   R3
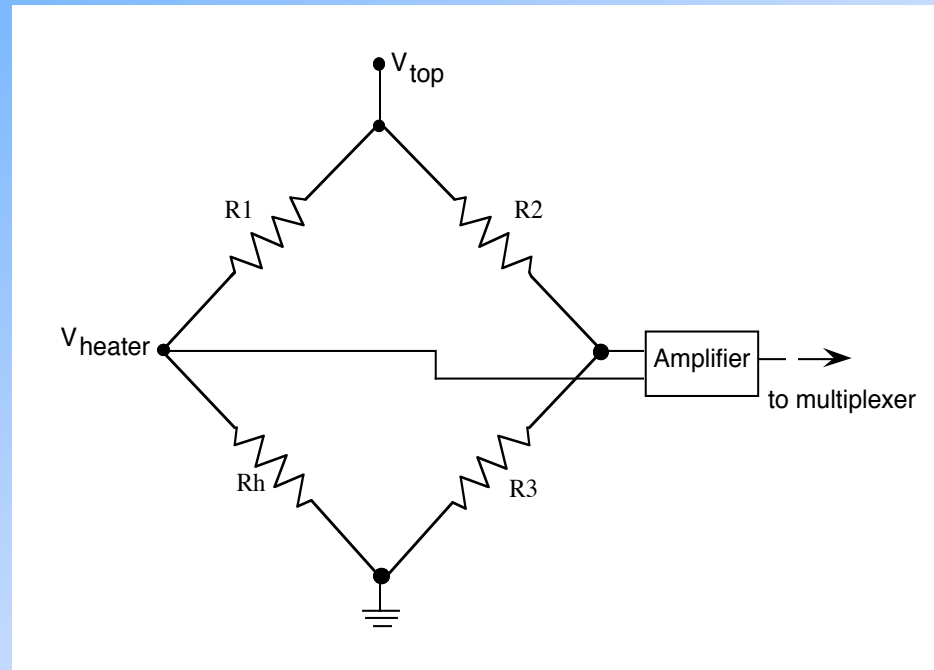
- **Heater resistance changes linearly with temperature**
- **R1 is chosen for each heater such that the *heat flux* is constant for all heaters in the array**
- **Heat flux does not change appreciably with changes in Rh**

Test Chamber

Pressure regulator

Compressed air

Stainless steel bellows

Viewports

Stirrer

Light

Window

FC-72

Microscale heater array

CCD camera

Not to scale

Fill port/vacuum

Filter
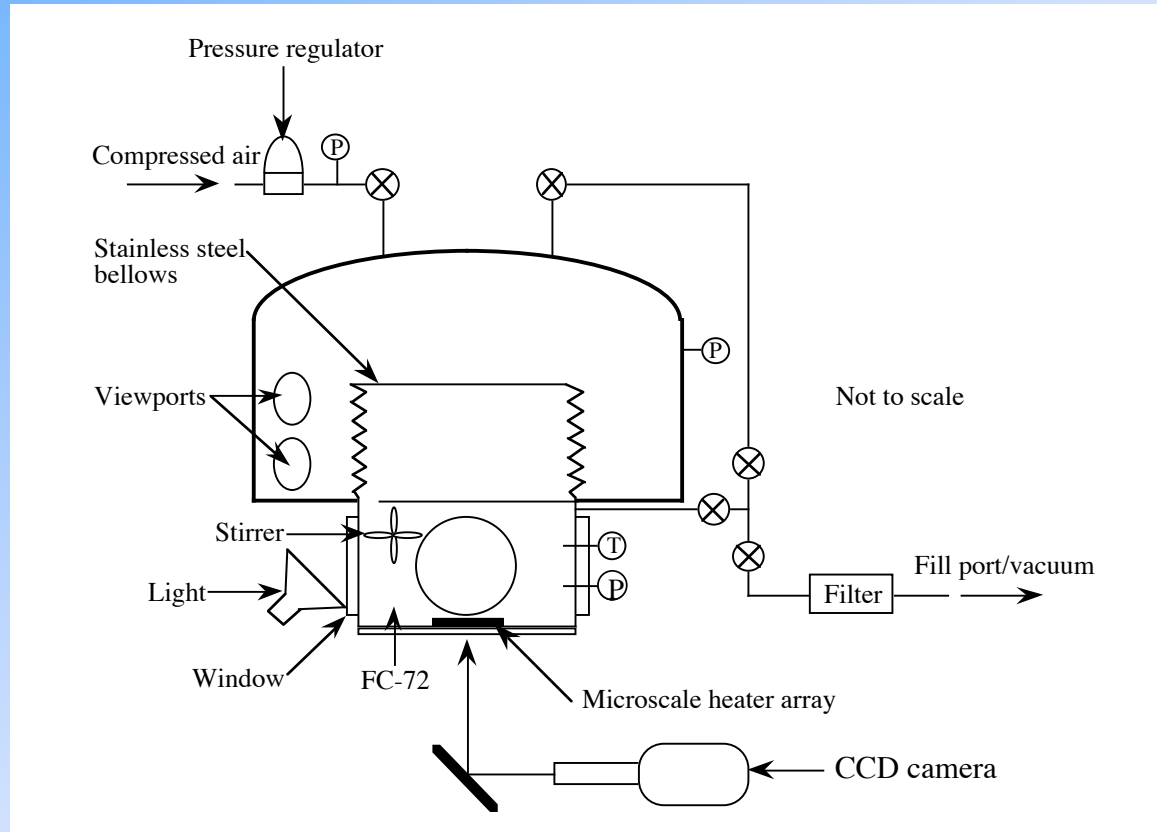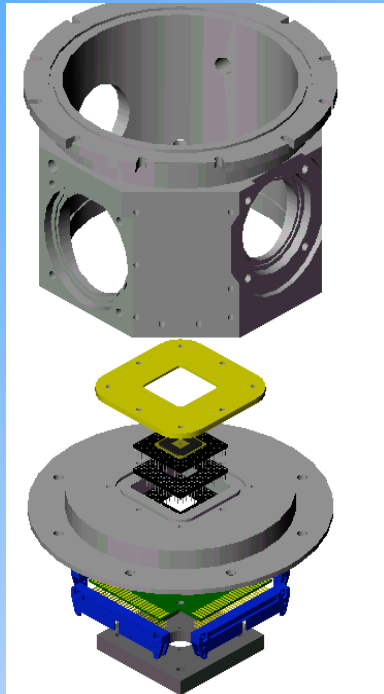
Experimental Results
(Earth Gravity)

Test Conditions for Constant Temperature Tests

- **Fluid: FC-72**

- **Pressure=1 atm (T_{sat}=56.7 °C)**

- **Wall temperature=76 °C**

- **Bulk temperature=52 °C, 41 °C**

Heat Transfer Variation During Single Bubble Event

1 mm
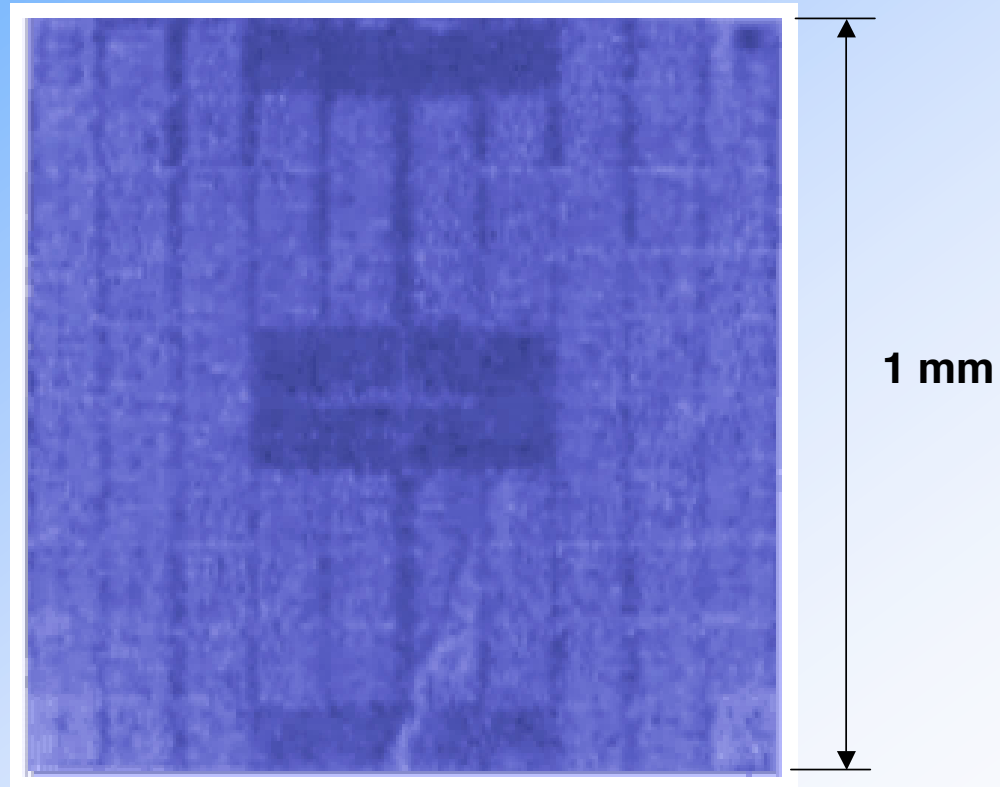
- **Tbulk=52 °C**

Single Bubble Heat Transfer
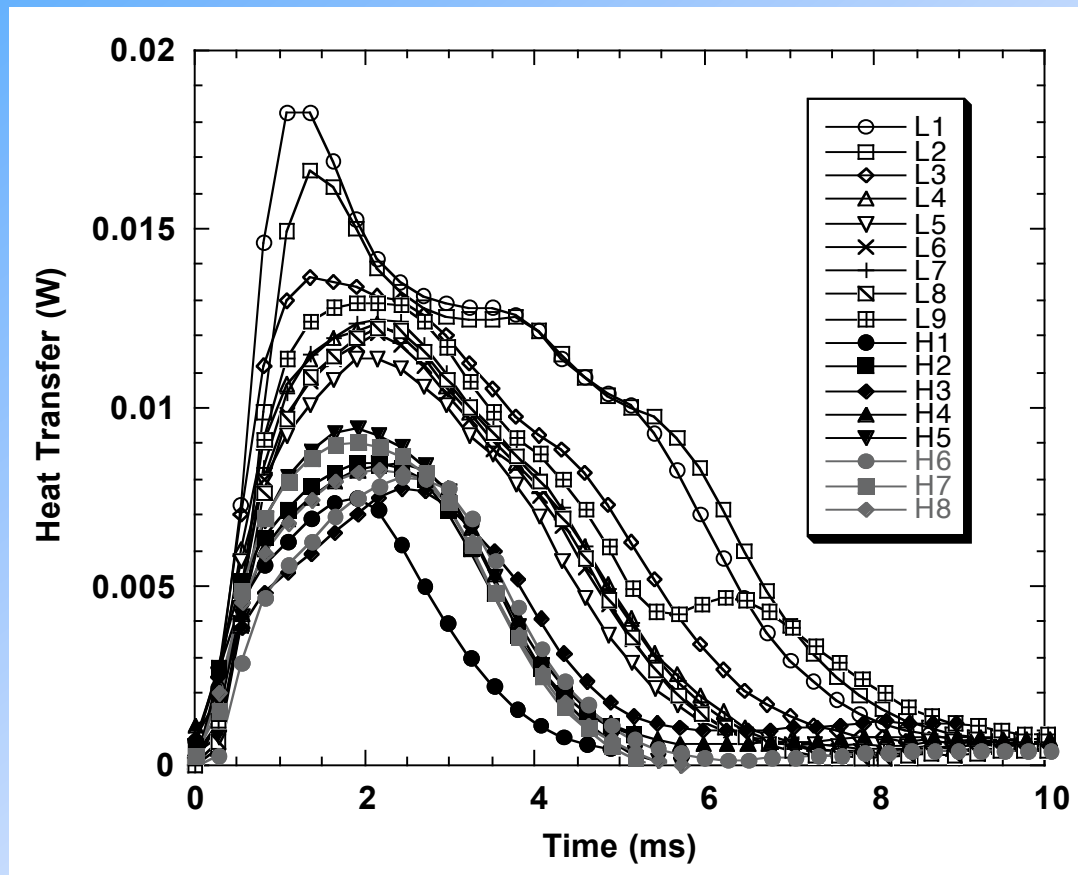
- **Change in heat transfer profile observed for low subcooling case–may be linked to changes in baseline heat transfer.**

Oscillating Bubble Heat Transfer

1 mm
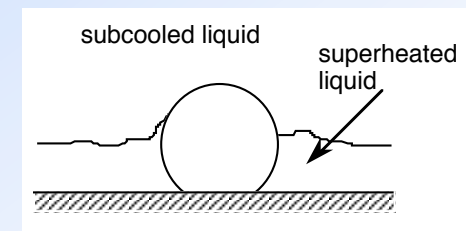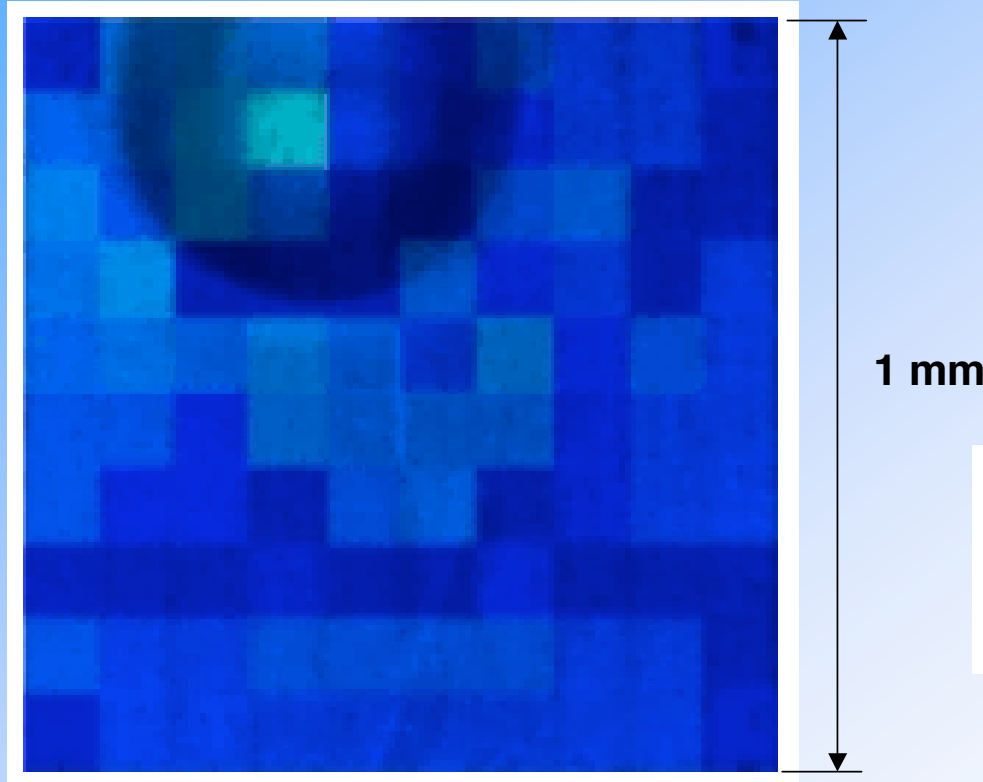
- Tbulk=41 °C
- Bubble oscillates in size due to changing balance between evaporation and condensation

Oscillating Bubble Heat Transfer
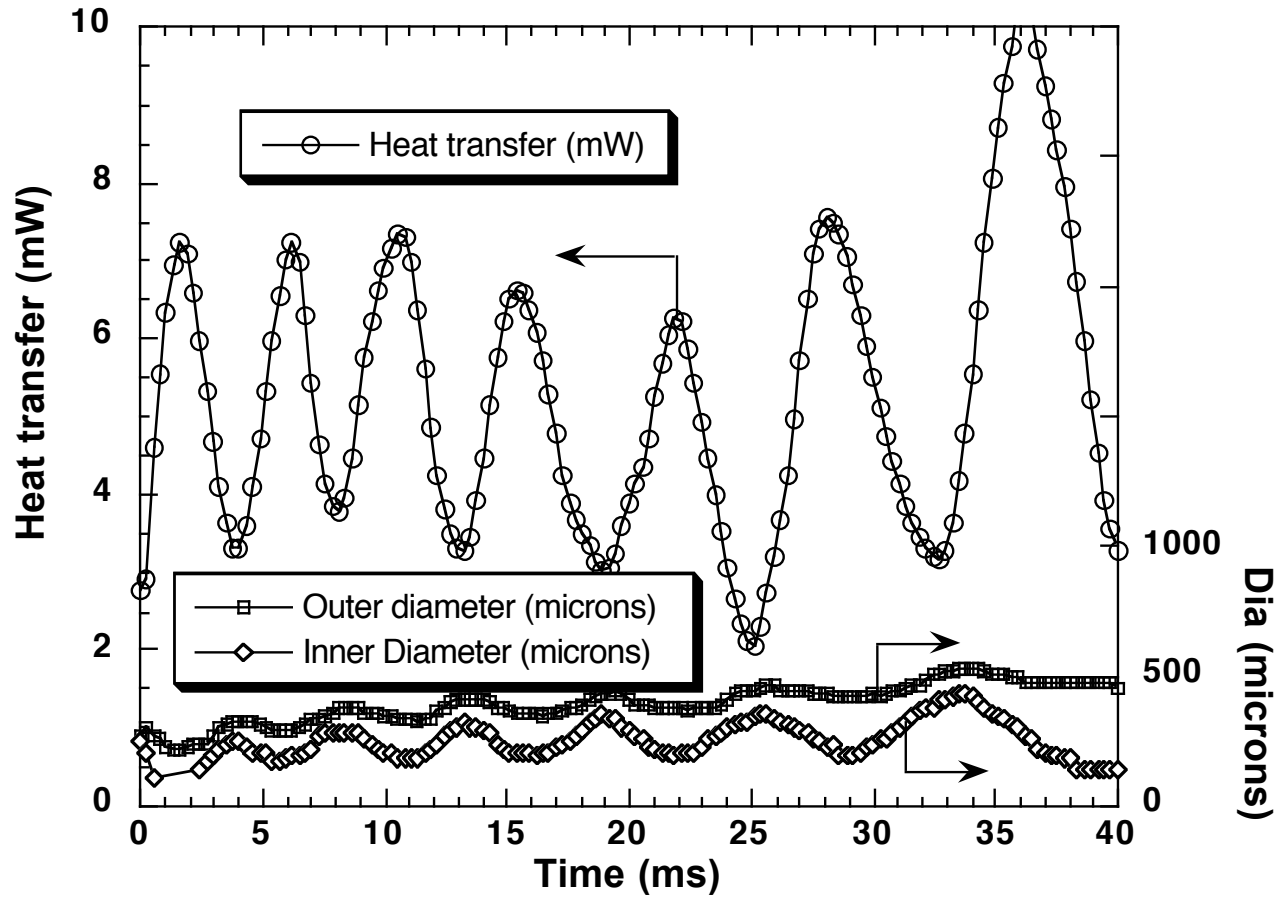
Contact Line Heat Transfer Under Sliding Bubble

1 mm
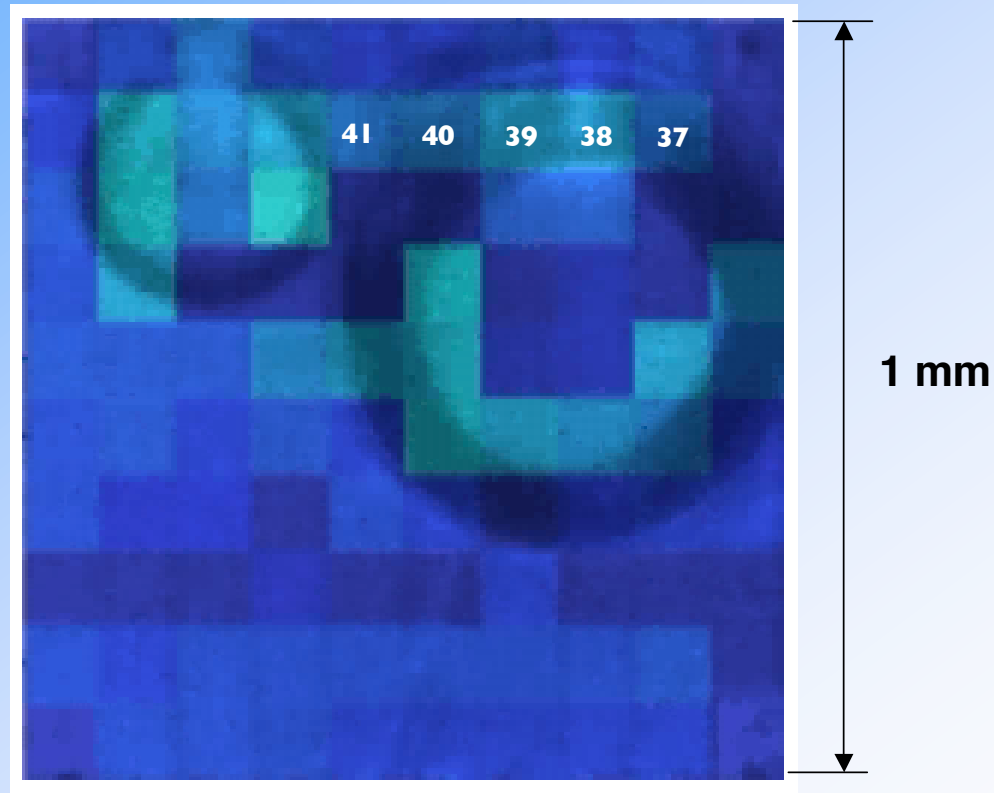
- Tbulk=41 °C
- Bubble velocity~2.2 cm/s

Contact Line Sliding Bubble Heat Transfer
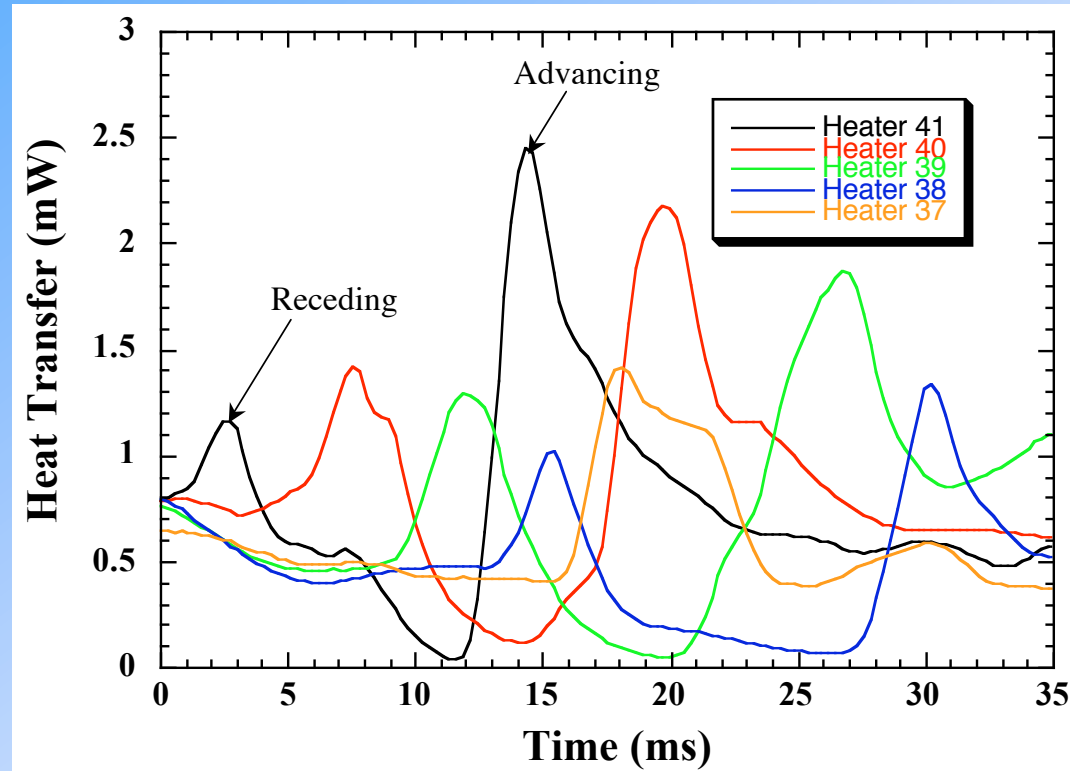
- **Higher heat transfer observed for advancing contact angle**

Transient Conduction Rewetting Model
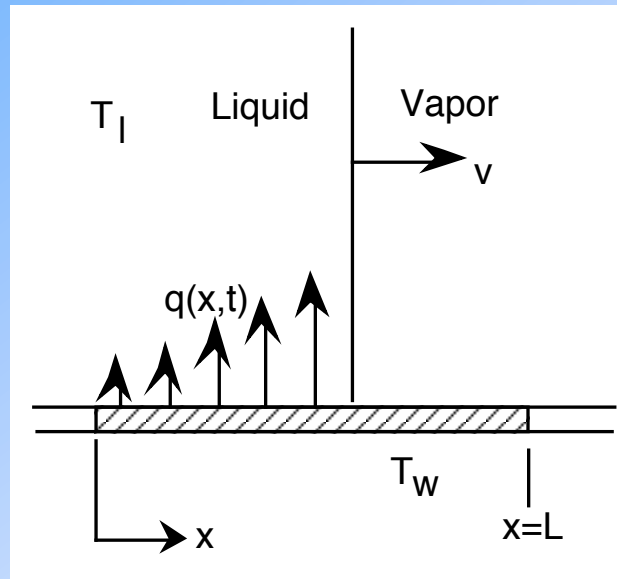
$$\dot{q}'' = \frac{k(T_w - T_l)}{\sqrt{\pi \alpha_l t}} \Rightarrow \dot{q}(t) = \frac{2k(T_w - T_l)}{\sqrt{\pi \alpha_l}} wv\sqrt{t}$$

- **Model given in Demiray and Kim, IJHMT (2004)**
- **Heater heat transfer proportional to wetting velocity v**

Measured vs. Predicted Heat Transfer
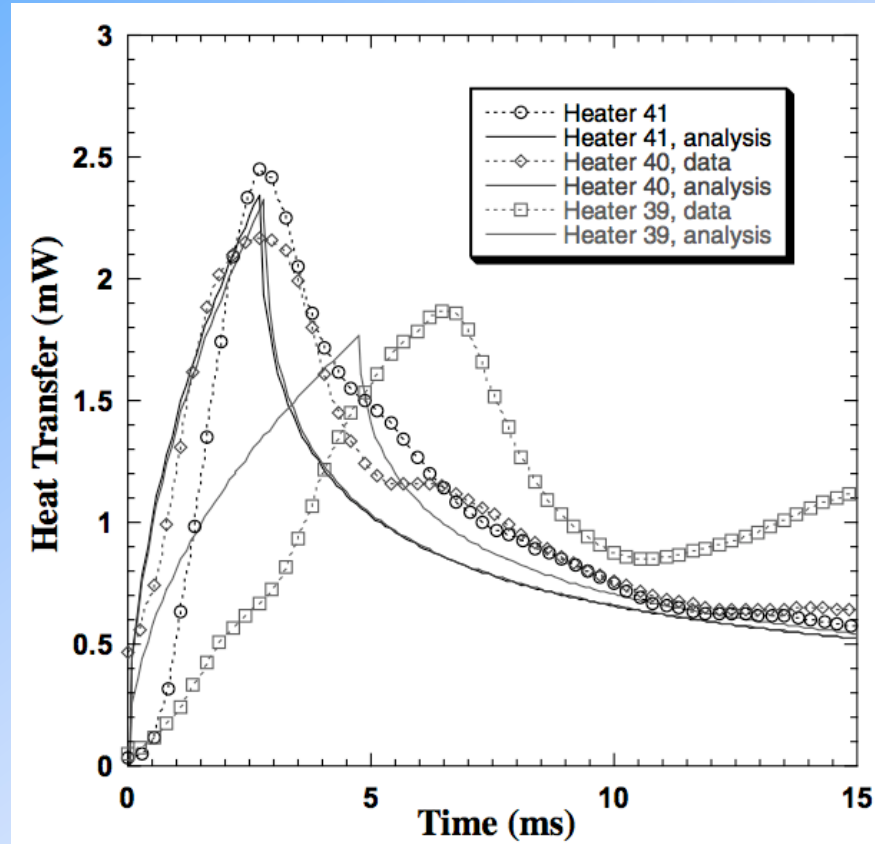
- Good agreement in location and magnitude of peaks in heat transfer.
- Good agreement in shapes of of curves.

Test Conditions for Constant Heat Flux Tests

- **Fluid: FC-72**

- **Pressure=1 atm (T_{sat}=56.7 °C)**

- **Bulk temperature=52.3 °C**

- **Applied voltage: 6.2 V to 8.3 V**

- **Average wall temperature: 90 °C to 110 °C**

  (Single bubbles, coalescing bubbles)

Applied Power Profile
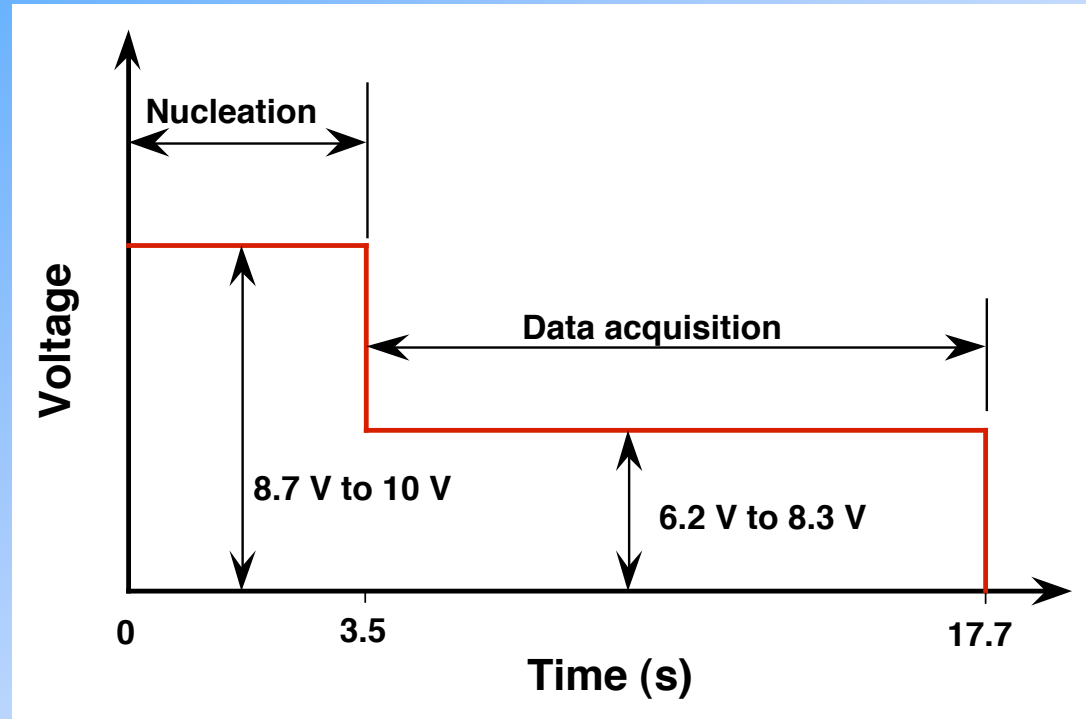
- Initial high voltage (8.7 V–10 V) applies for 3.5 s to initiate nucleation.
- Test voltages between 6.2 V and 8.3 V for 14.2 seconds.

Temperature Measurements
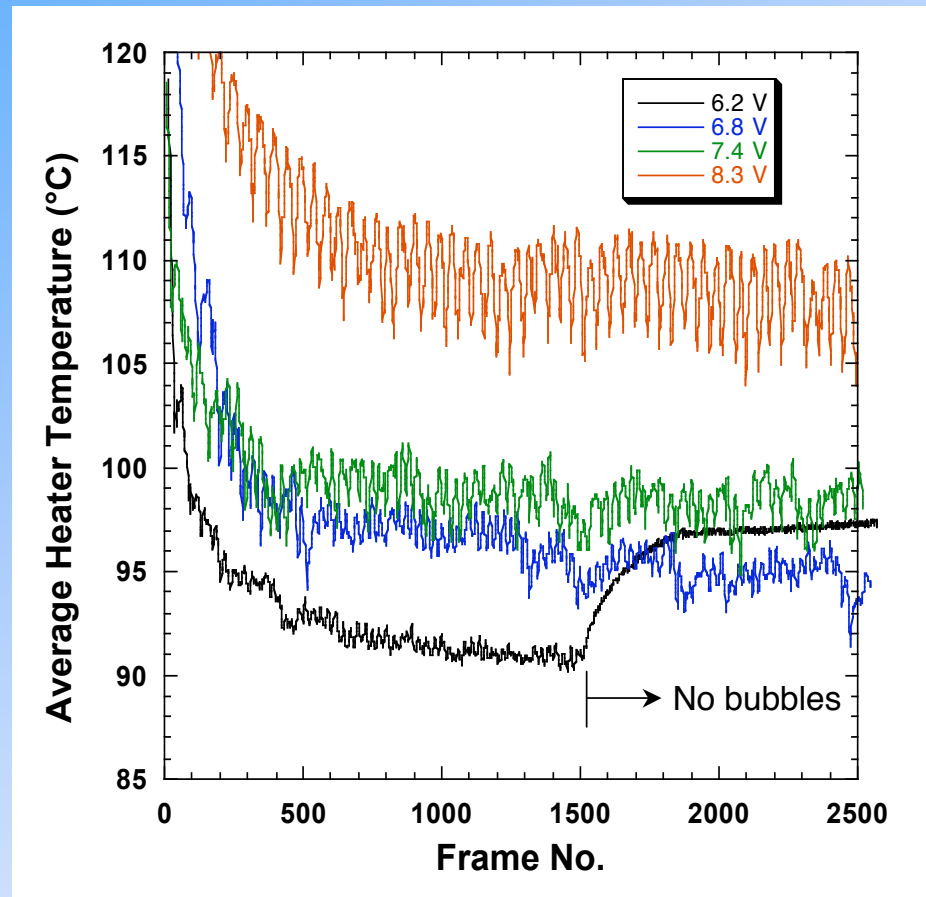
- **Data from each heater acquired at 1130 Hz**

Temperature Distribution Movie (6.8 V case)

Corresponding Temperature (°C)

80   90   100   110

730.09ms

1 mm

825

Case: pcb5 6p8v pp
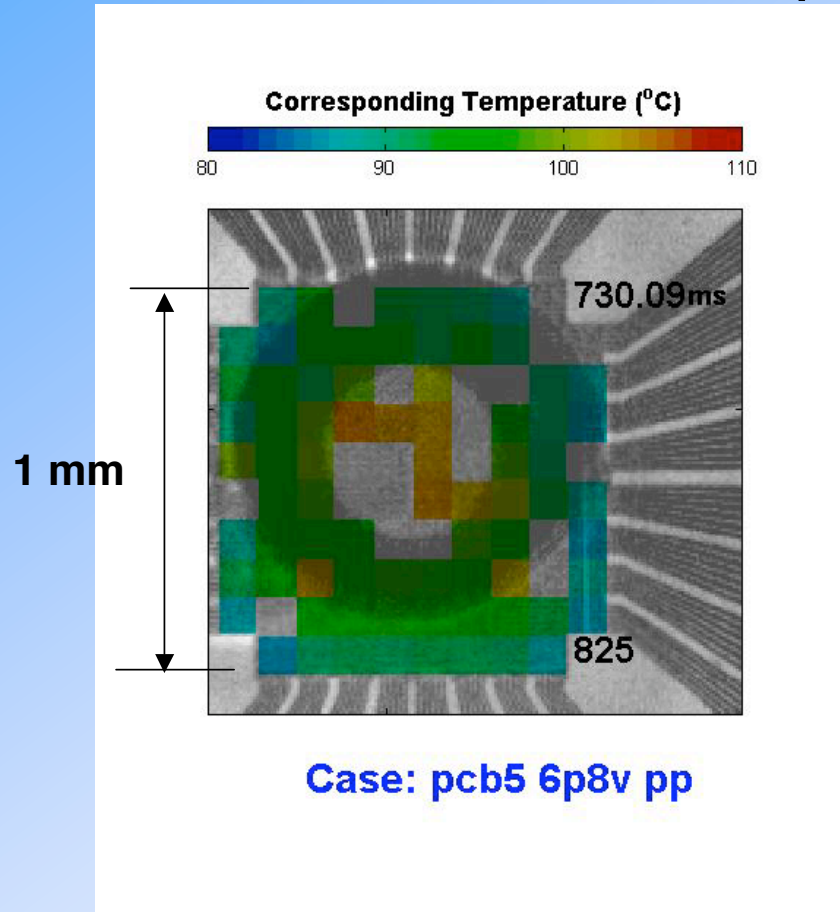
- Video acquired at 1130 Hz.
- Each heater is colored according to heater temperature.

Time Resolved Temperature Distribution During Bubble Nucleation and Departure (6.8 V case)
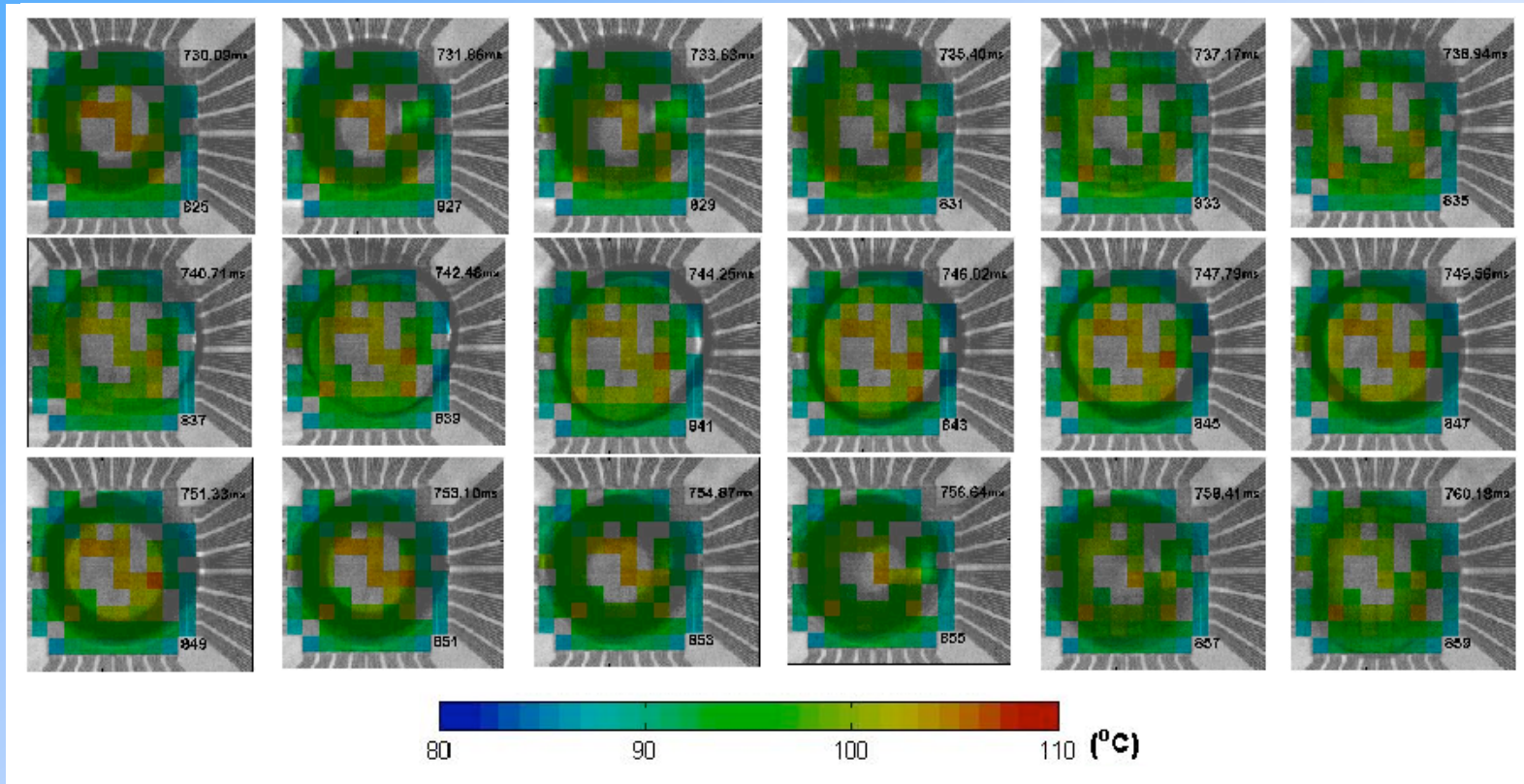
- **Images presented every other frame (565 Hz)**

Average Heater Temperature Variation (Single Bubbles)
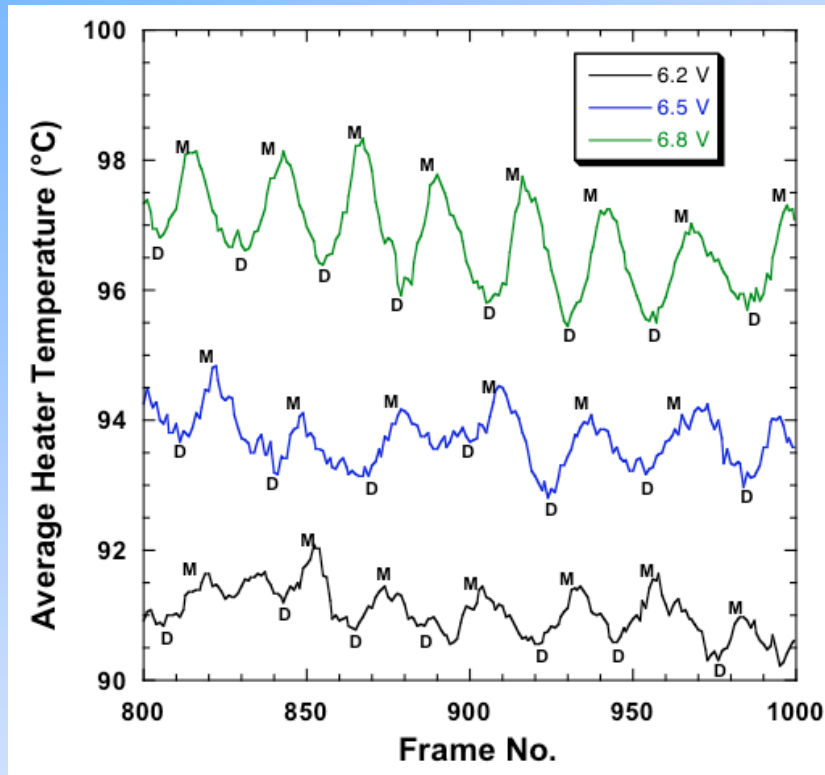
- Maximum temperature occurs when dry spot size is maximum (M)
- Minimum temperature occurs at bubble departure (D).

Time Resolved Temperature Distribution During Bubble Coalescence and Departure (7.1 V case)
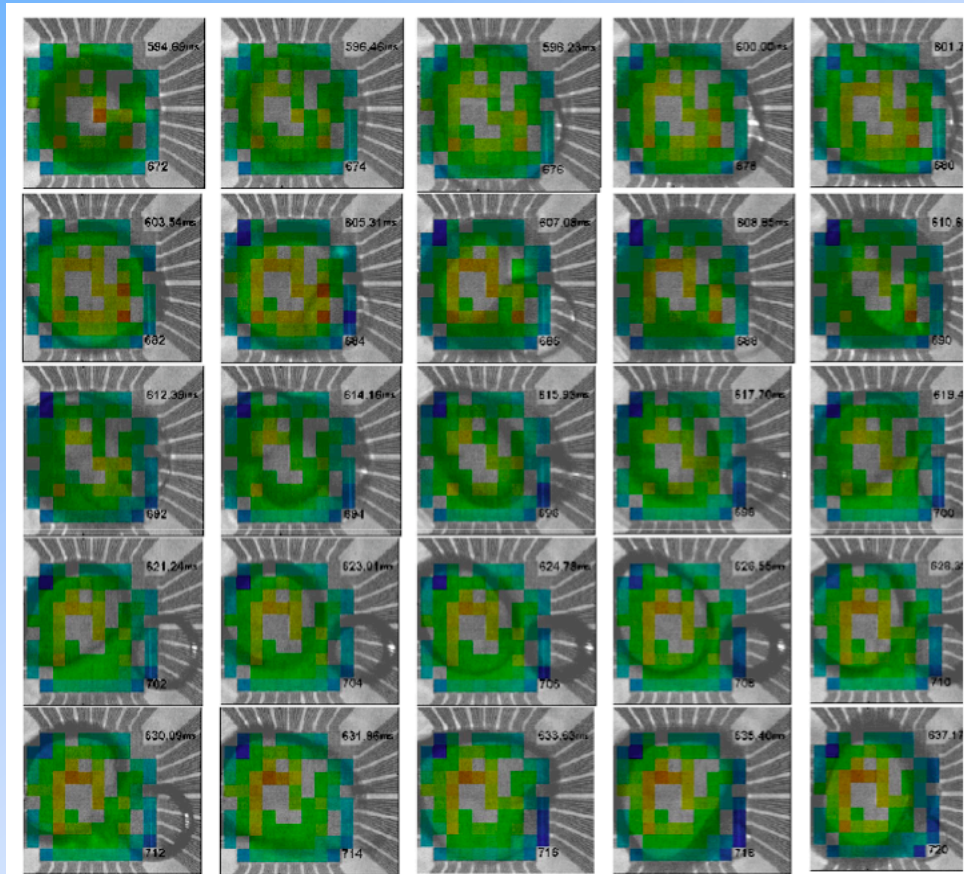
- **Images presented every other frame (565 Hz)**

Average Heater Temperature Variation (Bubble Coalescence)
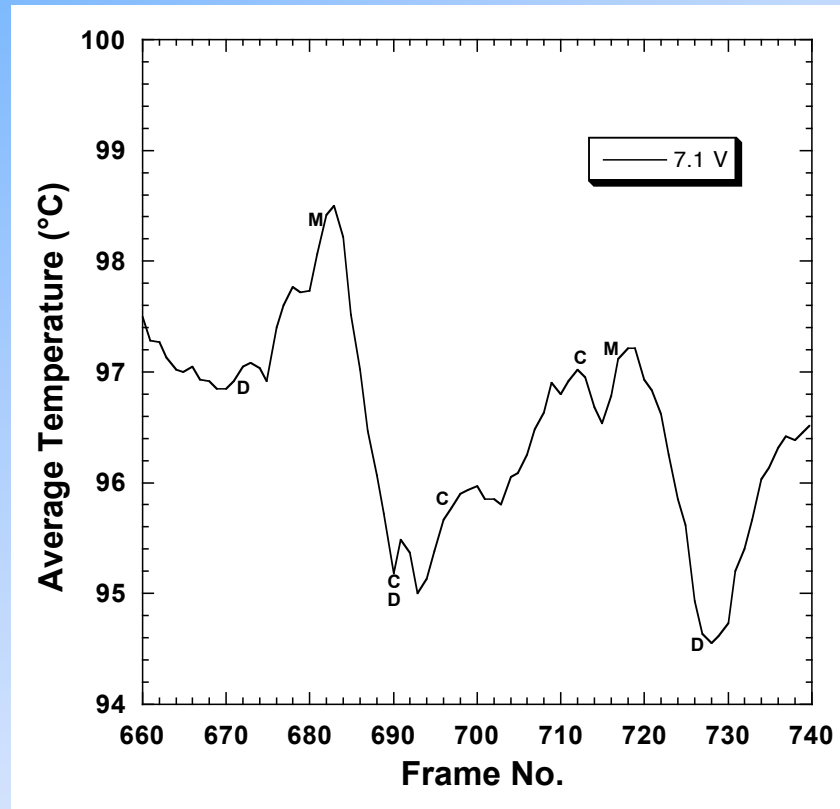
- **Bubble coalescence results in a small drop in wall temperature.**

Determination of Wall-to-Liquid Heat Transfer

- **Computational domain:**
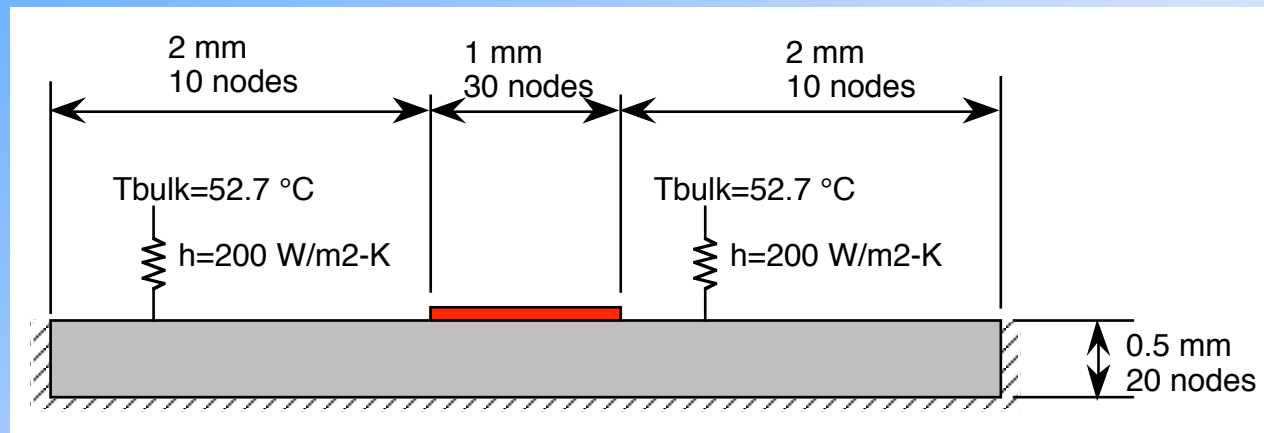
- **Compute temperature distribution within substrate at each time step after imposing heater temperature distribution on surface.**
- **Line-by-line TDMA with Gauss-Seidel iteration applied in all three directions**
- **Heat transfer into substrate was computed at each time step, then subtracted from supplied power to obtain heat transfer into liquid.**

Heat Flux Distribution Movie (6.8 V case)

Case: pcb5 6p8v pp
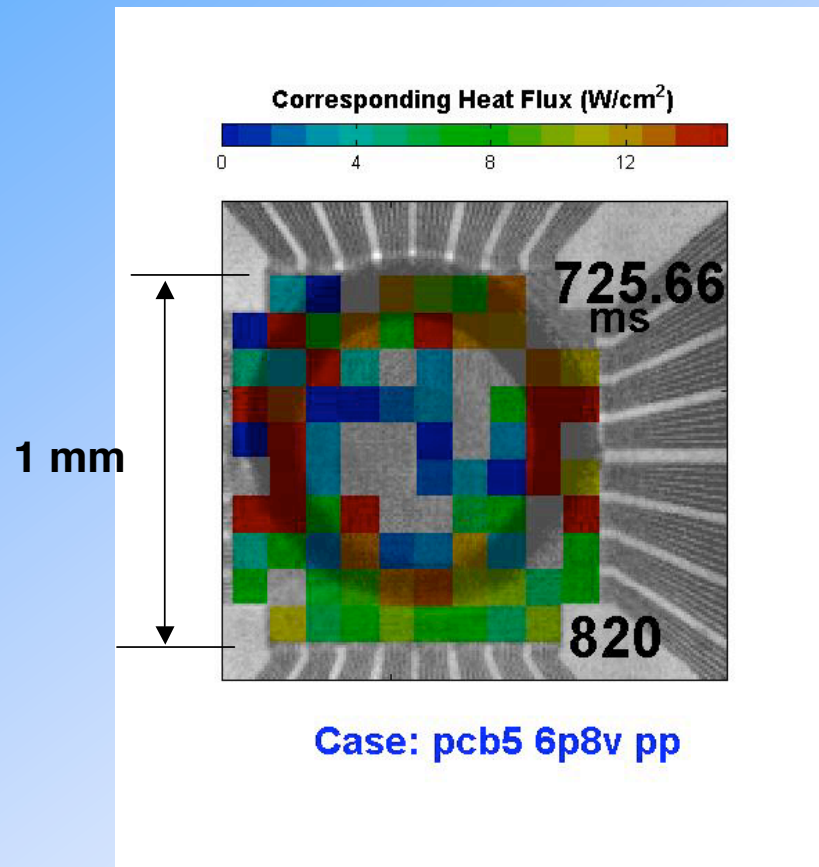
- **Video acquired at 1130 Hz.**
- **Each heater is colored according to heater heat flux.**

Time Resolved Heat Flux Distribution During Bubble Nucleation and Departure (6.8 V case)
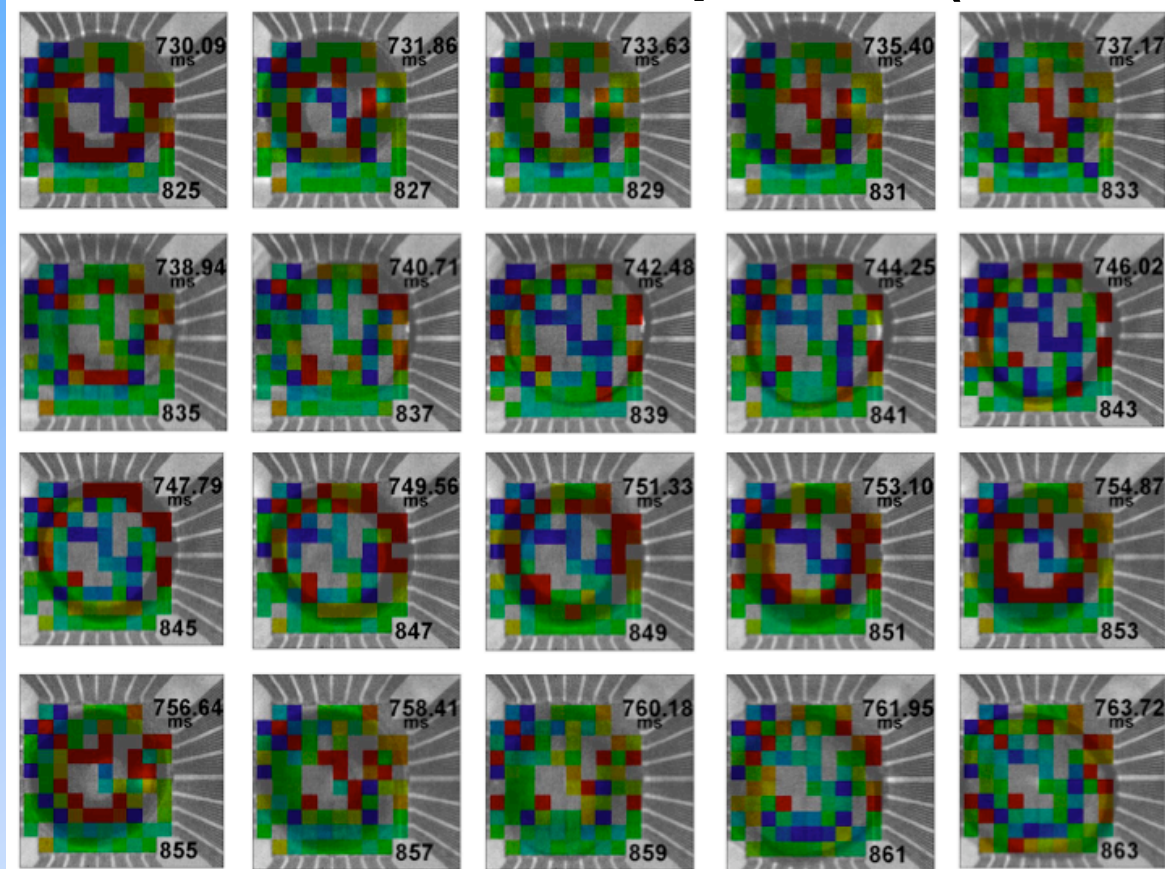
- **Images presented every other frame (565 Hz)**

Average Heat Flux Variation (6.8 V case)
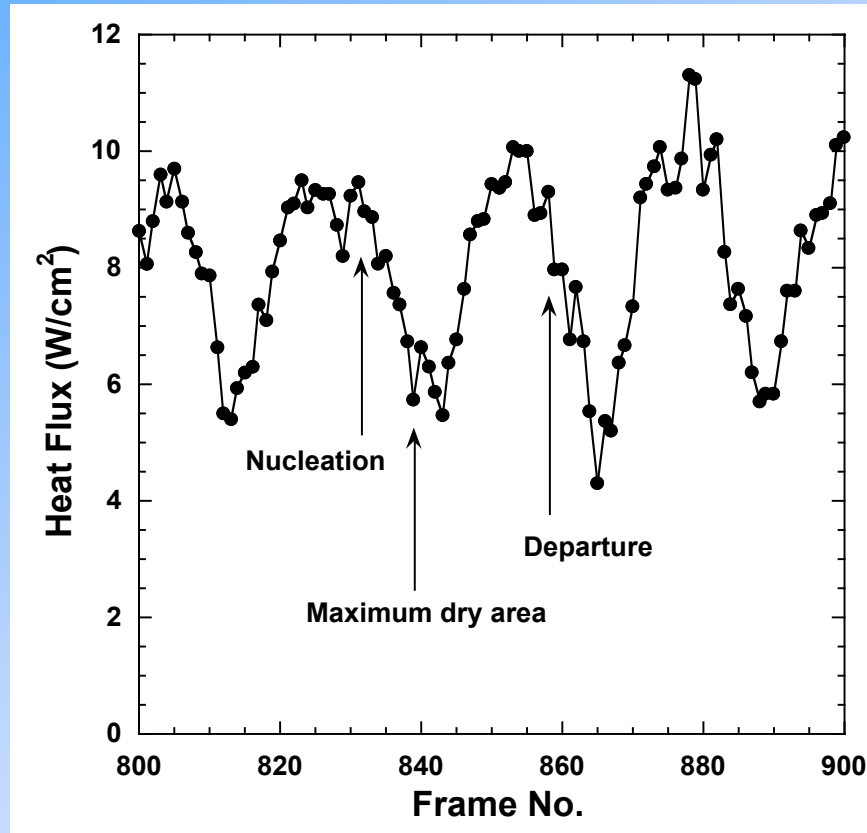
- **Minimum heat flux occurs when dry spot size is maximum (M)**
- **Maximum heat flux occurs at bubble departure (D).**

Average Heat Flux Variation (7.1 V case) (Bubble Coalescence)
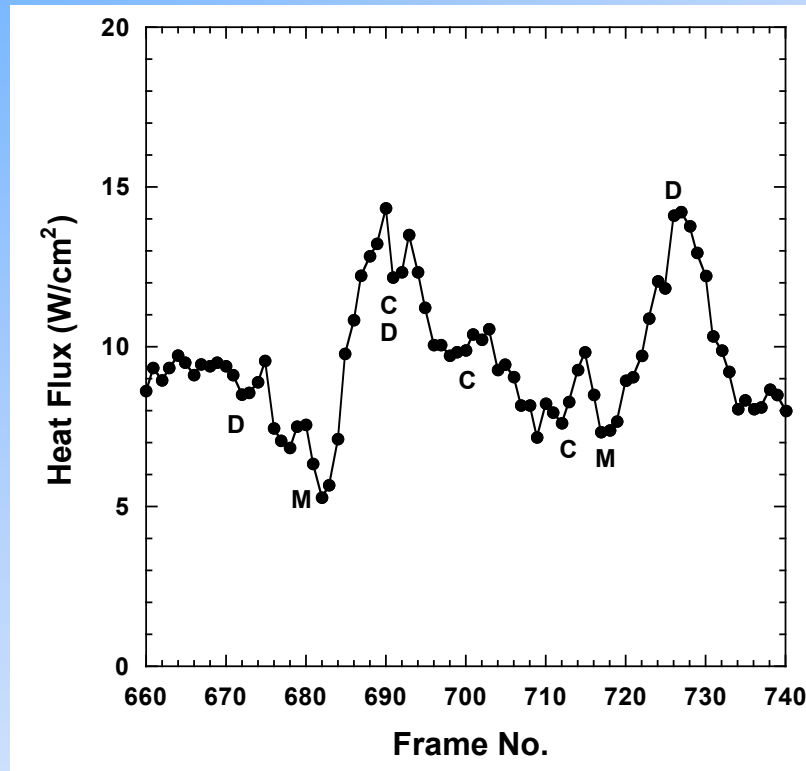
M: Maximum dry spot   **D: Bubble departure**
C: Coalescence event

Experimental Results (Low Gravity)

Test Conditions for Low-G Results

- **Fluid: FC-72**

- **Pressure=1 atm (T_{sat}=56.7 °C)**

- **7 mm heater array**

- **Bulk temperatures: 28 °C – 52 °C**

Low-Gravity Boiling Measurements (T$_{bulk}$= 28°C)

1.6 x 1.6 mm^2
(6 x 6 heaters)

7 x 7 mm^2
(10 x 10 heaters)
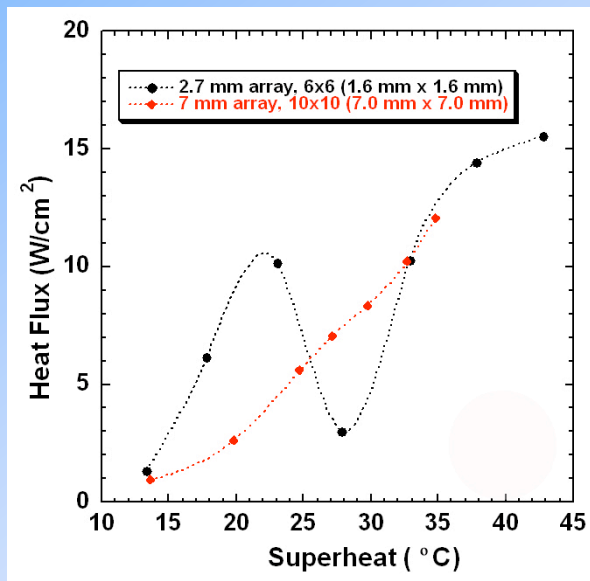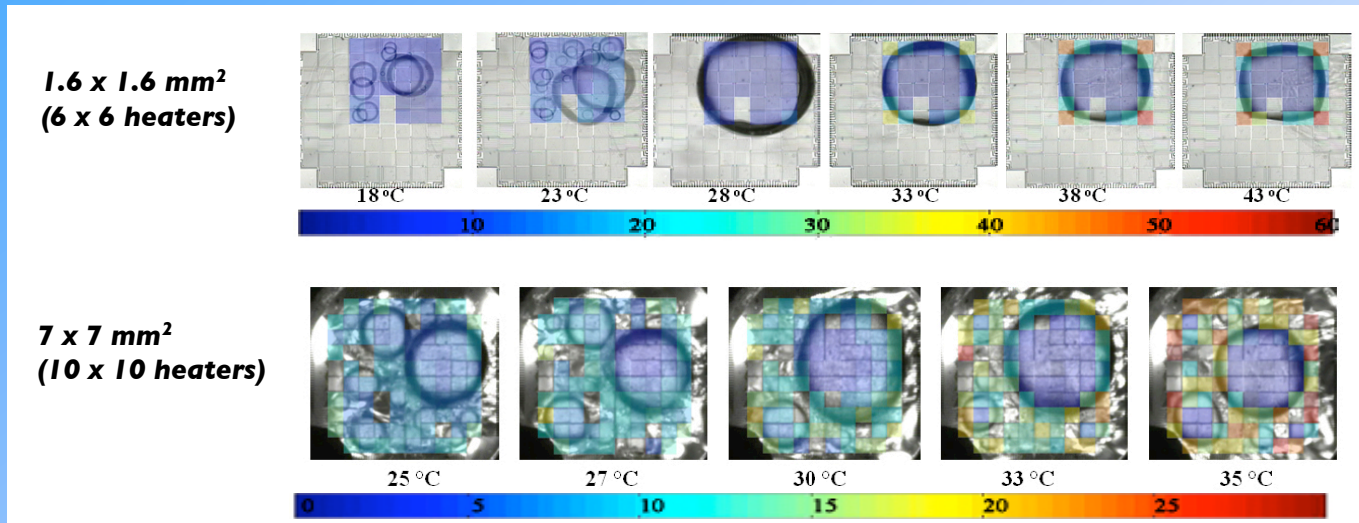
- **At low wall superheats, surface characteristics affecting nucleation site density appear to dominate the boiling curve behavior**
- **Boiling is dominated by thermocapillary convection at higher wall superheats**
- **Larger heaters (> 49 mm^2) may not dryout completely at higher superheats**

Aspect Ratio Boiling Observations (7 mm array)

$\Delta T_{sat} = 35°C$, $\Delta T_{sub} = 29°C$

1.4 x 2.8 mm², (2x4)   1.4 x 4.2 mm², (2x6)   1.4 x 5.6 mm², (2x8)
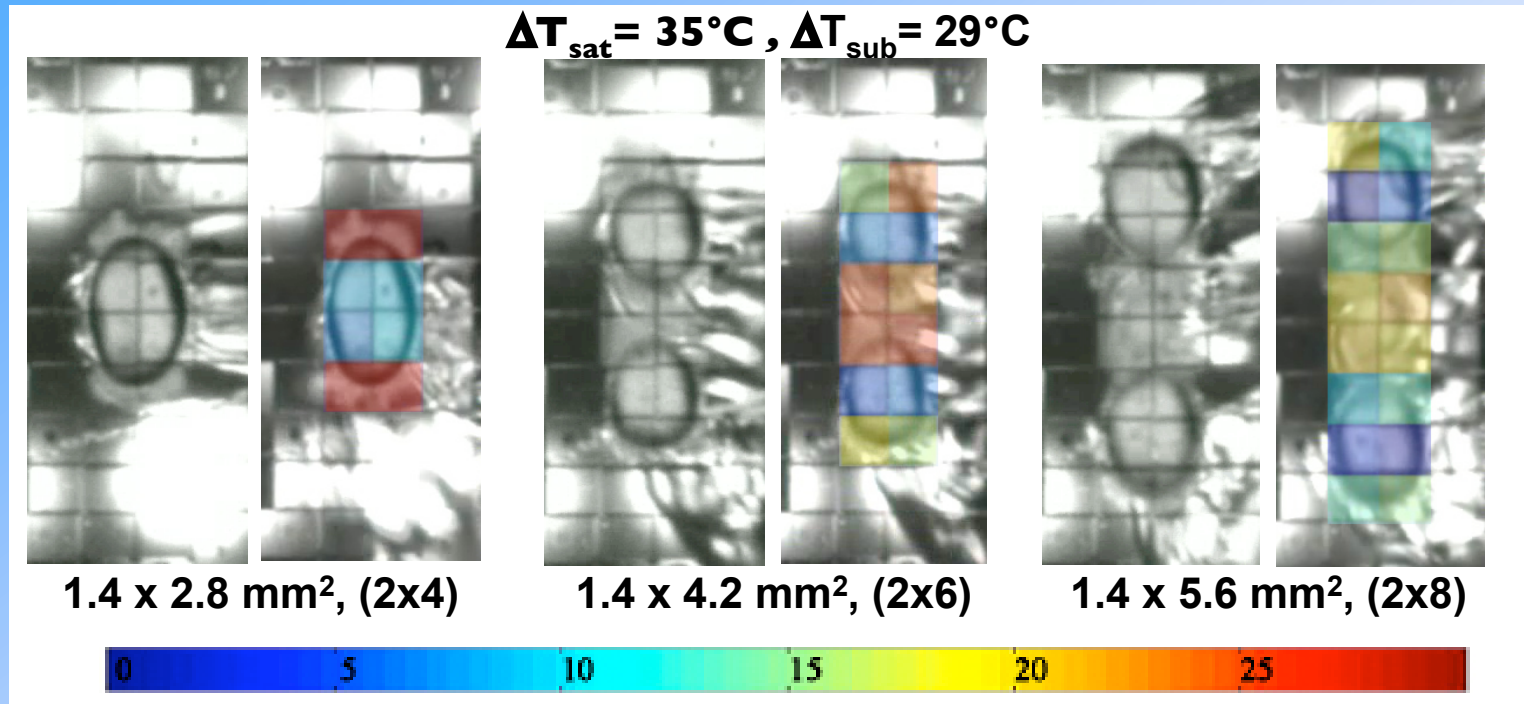
- **Strong influence of thermocapillary convection**
- **Surface tension wants to maintain a spherical bubble shape and can cause an increase in wetted area (compared to square heaters)**

Aspect Ratio (ΔT_{sub} = 28 °C)
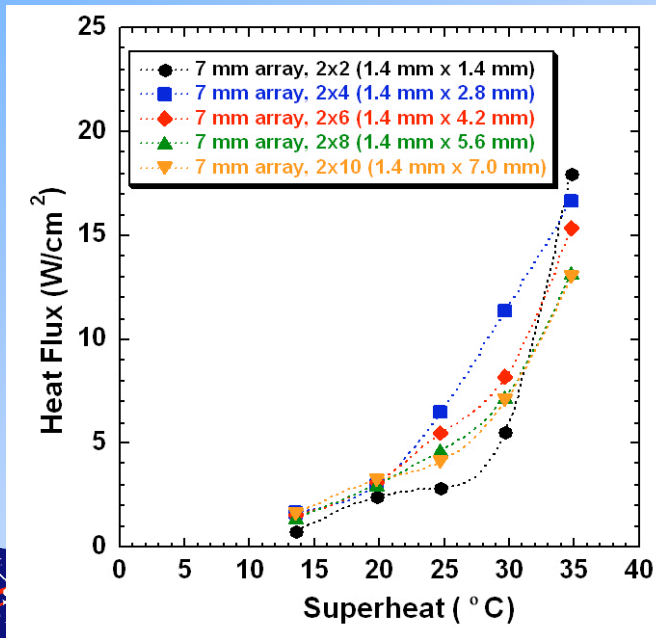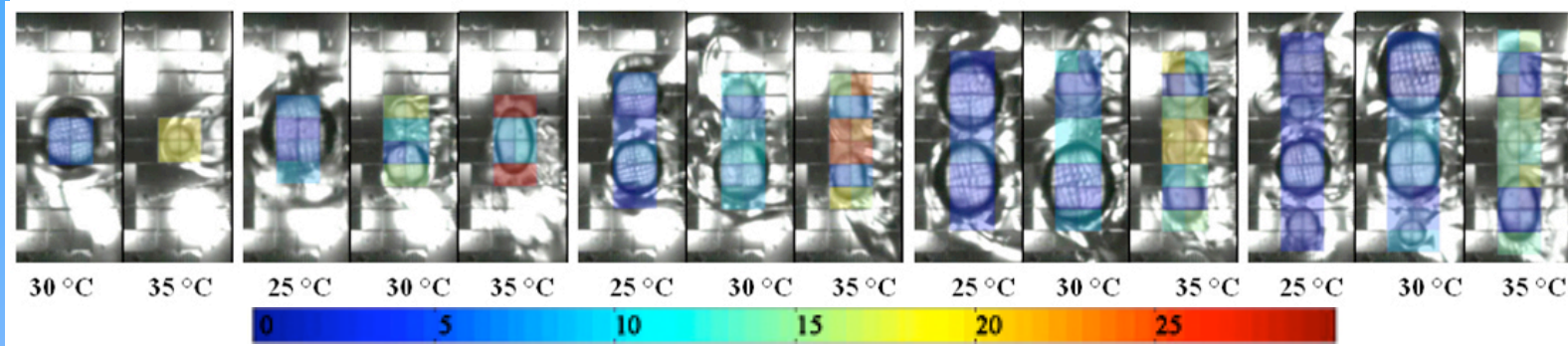
- **For a given wall superheat, the heat flux decreases with increasing aspect ratio**
- **Increasing two dimensionality of the thermocapillary flow field around the heater (increasing aspect ratio)**
- **Mechanisms that increase wetted area fraction**
  - **Thermocapillary effects**
  - **Surface tension**

Origin of Thermocapillary Convection
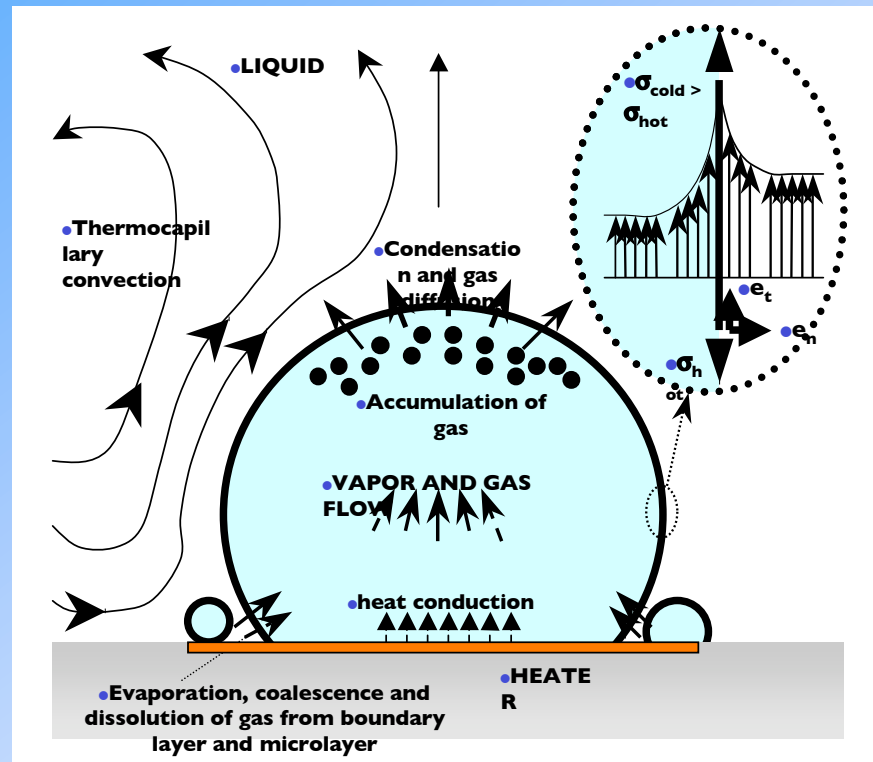
- **Thermocapillary flow results from surface tension gradients along an interface which can form due to:**
  - temperature gradients
  - material composition
  - electrical potential

FC-72 Characterization

Substance	M.W.	GC Area %	BP (°C)	
n-perfluorohexane	338	73.2	56	C6F14
perfluoro-2-methylpentane	338	17.892	57.66	C6F14
perfluoro-3-methylpentane	338	5.954	58.37	C6F14
perfluoro-2,3-dimethylbutane + perfluoro-2,2-dimethylbutane	338	1.723		
perfluorocyclohexane	300	1.105	50.61	
perfluoromethylcyclopentane	300	0.126	48	C6F12

- **Mass spectometry analysis was performed by Dr. Thomas Hartman at Rutgers University**

BXF/MABE Flight Experiment